



Study of Pulsatile Flow in Common Carotid Artery with Different Stenosis' Shapes within Various Wall Conditions

P. Bayat^{1,2} and M. R. Tavakoli^{2†}

¹ Department of Mechanical Engineering, York University, Toronto, M3J1P3, Canada

² Department of Mechanical Engineering, Isfahan University of Technology, Isfahan, 84156-83111, Iran

†Corresponding Author Email: mrtavak@cc.iut.ac.ir

(Received February 17, 2018; accepted August 13, 2018)

ABSTRACT

Recently, due to the development of CFD techniques, many attempts have been made to simulate the initiation and progression of atherosclerosis. In recent works, various curves have been suggested to model the stenosis shape. However, little effort has been made to study the importance of the stenosis shape on the flow behavior. In this study, four types of stenosis with asteroid, Gaussian, semi-circle, and sinusoidal shapes were simulated in order to study the effect of the stenosis shape on flow behavior and diagnosis parameters. Shear stress and flow behavior were investigated in the common carotid artery with stenosis severities of 30%, 40%, and 50%. Flow was assumed to be unsteady and the inlet to be a pulsatile flow. Two cases of Newtonian and non-Newtonian fluids were simulated. The no-slip and permeable boundary conditions were imposed on the outer walls. To examine the effect of the location of stenosis, modeling was conducted at various locations. The results showed that the maximum shear stress occurs in the Gaussian stenosis at the opening of the stenosis. Semi-circle, sinus, and asteroid shapes had the next largest shear stress values. Additionally, the location of stenosis had a negligible effect on the maximum shear stress. However, flow resistance increased with increasing the stenosis's distance from the beginning of the artery. This study indicates that stenosis shape highly affects the flow characteristics, and stenosis severity is not the only parameter that is important. Hence, the stenosis shape should be considered when simulating atherosclerosis.

Keywords: Pulsatile flow; Common carotid artery; Stenosis; Permeable walls; Newtonian fluid.

1. INTRODUCTION

Cardiovascular diseases are one of the most common causes of death worldwide. Atherosclerosis is a prevalent vascular disease. In the recent years, the development of CFD methods has caused numerous attempts to be made to simulate arteries and study streamlines and link them to the vascular diseases.

Blood consists of plasma, red and white blood cells, and platelets. Plasma constitutes the major part of blood and is a Newtonian and incompressible fluid with a density of 1.2 cP at 37 °C. However, blood cells and other components in the solution cause blood to have a non-Newtonian behavior. Volumetric ratio of red blood cells to total blood volume is known as hematocrit which is about 40-45% in a normal person (Sugihara-Seki and Fu (2005)). The larger an artery is, the blood behaves more like a Newtonian fluid (Perktold *et al.* 1999). In large blood vessels, blood behavior can be

assumed to be Newtonian with a good approximation, while in arterioles and venules, when diameter decreases, hematocrit decreases due to the Fahraeus-Lindqvist effect, and as a result, viscosity decreases. Therefore, in capillaries, blood must be considered as a two-phase solution of plasma and blood cells (Fung (2013)).

Marcinkowska-Gapińska *et al.* (2007) examined the viscosities of 100 blood samples and compared them with the viscosity of the Casson, Quemada, and Ree-Eyring non-Newtonian models. They indicated that the Quemada Newtonian model was the most similar model to blood.

Atherosclerosis is a disease related to large and medium-sized arteries, such as the carotid, coronary, iliac, femoral, and elastic arteries such as the aorta, which could be the origin of many cardiovascular diseases. Atherosclerosis can cause complications by restricting blood flow. Blockage in the coronary or the carotid arteries can be fatal. The general belief is

that rate of shear stress is the main determinant of the formation and continuation of the disease. Extensive research has been done on the modeling of vessel wall, in which, different conditions with different Newtonian and non-Newtonian models has been considered to investigate shear stress and formation of vortices. [Azer and Peskin \(2007\)](#) investigated blood flow in aortic arch, descending aorta, aortic bifurcation, anonyma, left common carotid, subclavian, brachialis, iliac, and femoral arteries using one-dimensional equations of momentum and mass and Womersley velocity profile.

[Razavi et al. \(2011\)](#) examined pulsatile flow in the carotid artery using a Newtonian model and six non-Newtonian models. Their results showed that the Power-Law model has a greater deviation compared to the other models, while Generalized Power-Law and Modified-Casson are more similar to the Newtonian flow. [Sadeghi et al. \(2011\)](#) investigated the intravascular stenosis severity and suggested that increase in stenosis severity affects wall shear stress, peripheral stress, and their amplitude and the angle between them. [Jahangiri, et al. \(2015a\)](#) investigated single and dual stenosis with 30%, 50%, 70%, and 80% severities and suggested that endothelial cells were damaged in the case of 70% severity.

Nutrient transport to the cells occurs at the capillary level. Therefore, the loss due to wall permeability should be considered for more accurate modeling ([Wake \(2005\)](#)). [Fatourae et al. \(1998\)](#) considered this permeability and studied pulsatile flow inside the carotid artery.

[Krejza et al. \(2006\)](#) measured age, weight, height, neck's length and circumference, blood pressure, and the diameter of the common carotid artery (CCA) and internal carotid artery (ICA). They suggested that the average diameters of CCA and ICA are smaller in women than men. The same values were used in the present study.

In the present study, blood flow in common carotid artery was simulated in COMSOL Multiphysics. The flow was assumed to be unsteady, and pulsatile flow was imposed as inlet boundary condition. The effects of shape of the stenosis on the maximum shear stress and flow behavior was investigated. Two boundary conditions were imposed on the outer wall: permeable wall, and non-slip condition. In one case, blood was considered as a Newtonian fluid, and in the other case, it was considered as a non-Newtonian fluid with the Carreau model. The flow governing equations, geometry, and boundary conditions are presented in the following sections. Finally, results and the effects of stenosis' shapes on the flow parameters were studied.

2. THEORY

The behavior of blood can be assumed Newtonian in carotid artery due to its relatively large diameter. In this case, the flow governing equations will become the famous equations of continuity and Navier-Stokes:

$$\rho \frac{\delta u}{\delta t} + \rho(u \cdot \nabla)u = \nabla \cdot \left[-\rho I + \mu \left(\nabla u + (\nabla u)^T \right) \right] + F \quad (1)$$

$$\rho \nabla \cdot u = 0 \quad (2)$$

Where, u is the velocity vector, p is pressure, τ is the viscous stress tensor, F is the external body forces vector exerted on the system, which was assumed to be zero, ρ is the blood density which was considered to be 1050 kg/m³, and μ is the viscosity of blood which was considered to be 0.0035 Pa.s in the case of Newtonian blood.

The FEM method in Comsol Multiphysics was used to solve the equations, and the governing equations were discretized using the backward difference method.

In the first case, free triangular elements were used for geometrical mesh generation. The number of elements varied in different stenosis severities. First, 8000 free-form triangular elements were defined to solve the problem in the computational domain. For more accurate modeling, a finer mesh was used at the areas surrounding the stenosis wall to inhibit the high gradients.

Finer meshes were also examined to study the grid dependency. With about 16000 nodes, flow field and shear stresses were independent of the number of elements with good approximation. The absolute tolerance to control the absolute error was considered to be 0.001. The equations were solved for 4 cycles to ensure a periodic flow. The results reported in the following sections are corresponding to the fourth cycle.

2.1 Geometry and Boundary Conditions

Since the artery was considered as a tube, and the stenosis was modeled as cuts with different shapes around the tube, the problem was considered to be axisymmetric. Three-dimensional modeling was avoided to simplify the solution process, and instead, a two-dimensional axisymmetric problem was solved.

To study the effect of lipid accumulation on the maximum shear stress and flow behavior, four different types of stenosis were modeled: asteroid, semi-circle, Gaussian, and sinus (Fig.1).

In Fig. 1, the radius R was assumed to be 3.26 mm according to the data provided by [Krejza et al. \(2006\)](#). The location of stenosis was considered at a $K \times R$ distance ($K=3, K=5$) from the beginning of the artery. To better investigate the effects of these four types of stenosis, the value m , which represents the stenosis severity percentage, was considered to be 0.3, 0.4, and 0.5 which show 30%, 40%, and 50% severities.

The pulses used in this paper for the inlet boundary condition was the carotid artery pulse reported by [Fatourae et al. \(1998\)](#), and was obtained by a fitting harmonic functions (Fig. 2).

Fully developed flow velocity profile was used for the inlet boundary condition:

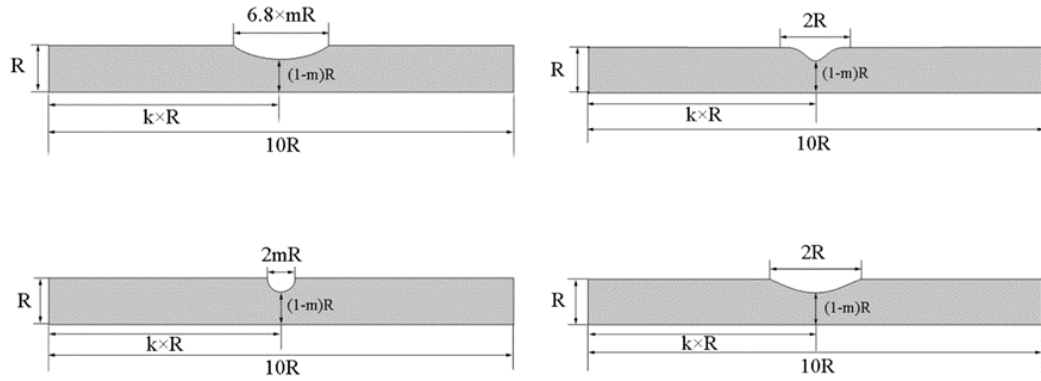


Fig. 1. Stenosis geometry from the top asteroid, semi-circular, Gaussian, sinus.

$$u(r, t) = 2\bar{u}(t) \times \left(1 - \left(\frac{r}{R} \right)^2 \right) \quad (3)$$

Where, \bar{u} is the average pulsatile velocity in the inlet section (Fig. 2).

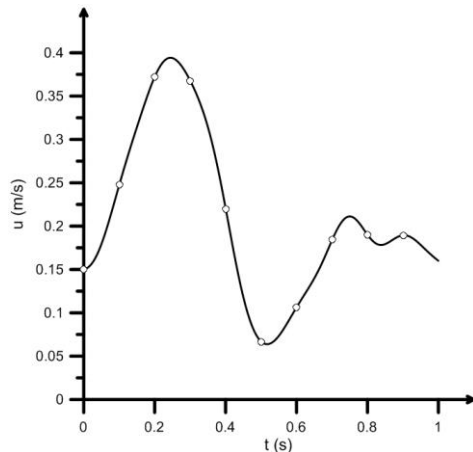


Fig. 2. Inlet velocity boundary condition.

In order to validate our simulation we compared our result with the numerical result of [Karimi et al. \(2013\)](#). Figure 3 indicates that there is acceptable consistency between the result of their result and our result.

3. RESULTS AND DISCUSSION

3.1 Effect of Boundary Conditions

According to the CFD theory and Navier-Stokes equations, only the pressure gradient appears in the equation, and the inlet and outlet pressure values do not affect the flow field and the stress. Therefore, according to Poiseuille's law, the only boundary condition affecting the results is the inlet velocity boundary condition.

$$\Delta p = \frac{8\mu L Q}{\pi r^4} \quad (4)$$

Inlet velocity directly affects the stress distribution

and flow field. Figure 4 shows the plots of the wall shear values at different times in the sinus stenosis with 40% stenosis severity in 3R distance from the beginning of the artery. Maximum shear stress occurred at 0.25 s, which is the peak time of the pulse. As expected, the location of the maximum shear stress is at the stenosis where the flow cross section reaches its minimum.

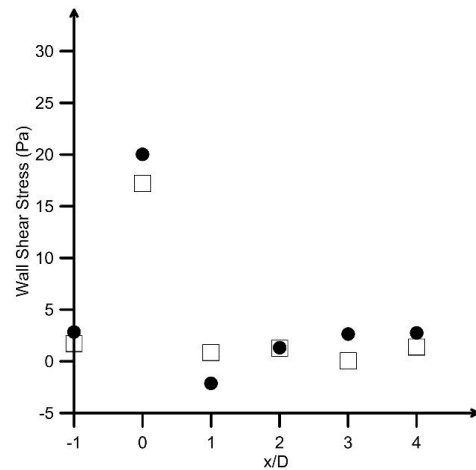


Fig. 3. Numerical validation.

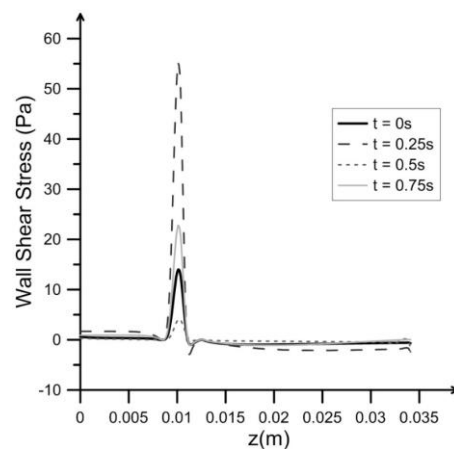


Fig. 4. Wall shear stresses in semi-circle stenosis with 40% stenosis severity at the 3R distance from the beginning of the artery.

The trends of the diagrams are similar in all times. Upon reaching the location of the stenosis and with increase in the shear stress rate, viscous shear stress suddenly increases and does not change much afterwards. This maximum shear stress value can have an important role in damaging the endothelial cells. Fry (1968) showed that shear stress values greater than 40 Pa can damage the endothelial cells. According to Ramstack *et al.* (1979), shear stresses greater than 100 Pa can cause detachment of endothelial cells, which in turn may result in the formation of blood clots. In a non-stenotic artery, the maximum shear stress is about 2 Pa (corresponding to the peak of the inlet pulse) that should not cause problems for these cells. But, with reduction in the flow cross-sectional area, the shear stress increases and can be dangerous. Figure 5 shows the non-stenotic case.

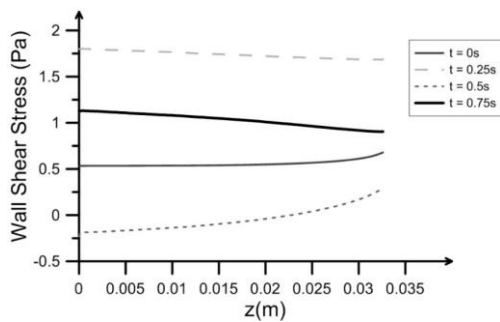


Fig. 5. Wall shear stresses without stenosis.

Permeable wall boundary condition (Eq. (5)) and the normal filtration rate (according to Fatourae *et al.* (1998)) were used to ensure that the walls permeability has negligible effect on the results.

$$v(R, t) = V_w = 4 \times 10^{-4} \text{ cm / s} \quad (5)$$

Comparing the results with the results of the no-slip boundary condition showed a negligible difference between them (in the order of 0.01 and lower) which shows that it can be ignored in the modeling. The results reported in the following sections were obtained when the no-slip boundary condition was applied.

3.2 Effect of the Stenosis Shape

The aim of this study was to investigate the effect of stenosis shape, which represents the accumulation of lipids within vessels, on the flow characteristics. All four types of the studied stenosis blocked the blood flow with the same degree; however, their slopes and curvatures were different. Figure 6 shows the diagrams of the wall shear stresses in both cases of stenosis at the distances of 3R and 5R from the beginning of the vessel. In all cases, the maximum shear stress occurred at the entrance of the stenosis. In both cases (3R and 5R distances), in 30% severity, the maximum shear stress was associated with Gaussian stenosis followed by semi-circle, asteroid, and sinus stenosis.

Stenosis with 40% and 50% severities were exactly

similar to the 30% case. Gaussian stenosis was significantly different from other models when the stenosis severity was increased. Sinus and asteroid stenosis had a negligible difference at 30% severities, however, their difference increased in 40% and 50% severities. The reason is that with increasing severity in the asteroid shape, the slope of the curve decreases, and the flow path becomes smoother.

The shear stress of 40 Pa can initiate the damage to the endothelial cells. As can be seen in the figure, cells are prone to damage in all 30, 40 and 50% severities in the Gaussian stenosis. However, in the three other shapes, the cells are not damaged in the 30% severity. By increasing the severity to 40%, maximum shear stress in semi-circle stenosis exceeded 40 Pa, whereas, it was about 40 Pa in sinus stenosis and less than 40 Pa in asteroid stenosis. In the case of 50% severity, maximum shear stress in all four shapes exceeded 40 Pa which can damage the cells that in a normal non-stenotic artery, tolerate at worst 2 Pa shear stress.

Stresses more than 100 Pa causes cell detachment and blood clots. This occurred only in the Gaussian curve with 50% severity. This value was about 90 Pa for the semi-circle curve which increased by increasing stenosis severity and exceeded 100 Pa. Therefore, in this case, blood clots are formed, which causes the platelets to repair the damaged area, resulting in increases in the blockage of artery.

Figures 7 to 9 show axial velocity in throat and poststenotic region at the time of maximum flow rate. It is shown that the maximum velocity at the stenosis exceeds 1m/s in the cases of 40% and 50% stenosis severity which is beyond the normal mode and might cause disorder in circulatory system (Jahangiri, Saghafian, and Sadeghi 2015b). Also, it could be seen that in all cases reverse flow can be predicted after the stenosis.

3.3 Effects of Location of the Stenosis

The next aim of this paper was to investigate the effect of location of stenosis on the results. Same stenosis severities were considered in two locations. As seen in Table 1, location of stenosis did not affect maximum shear stress significantly.

To investigate the effects of inlet velocity profile (in the first group of cases, parabolic velocity profile was imposed at the inlet), we solved again the problem for the flat inlet velocity profile. The results are shown in Table 1. Results show that in both cases, *i.e.* flat profile and parabolic profile, location of stenosis had a negligible effect on the maximum shear stress. It should be noted that the flow patterns considerably affect stress values, and in addition to the stenosis form and shape, stenosis severity directly affects streamlines as well. Streamlines in all cases are shown in Fig. 10. The values are plotted at the peak of inlet pulse ($t = 0.25$ s). In 30% severity, streamlines were smooth particularly in the sinus and asteroid stenosis, however, in 30% and 40% severities, more irregularities were present.

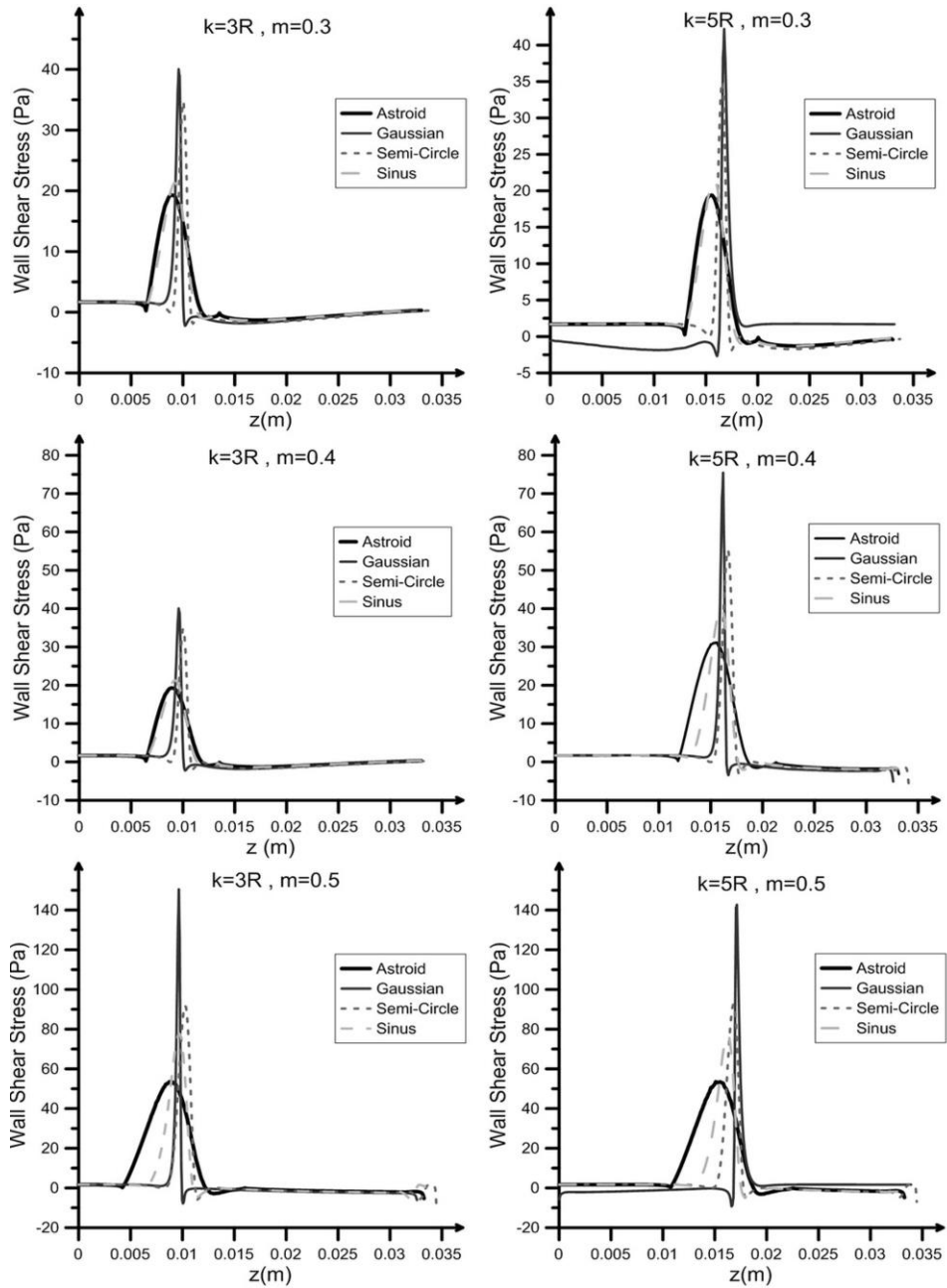


Fig. 6. Wall shear stresses in all shapes of stenosis.

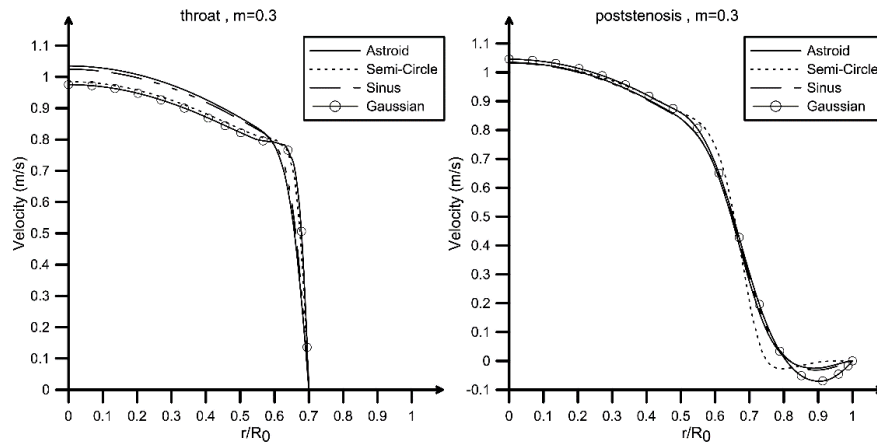


Fig. 7. Axial Velocity in all shapes of stenosis for $m=0.3$.

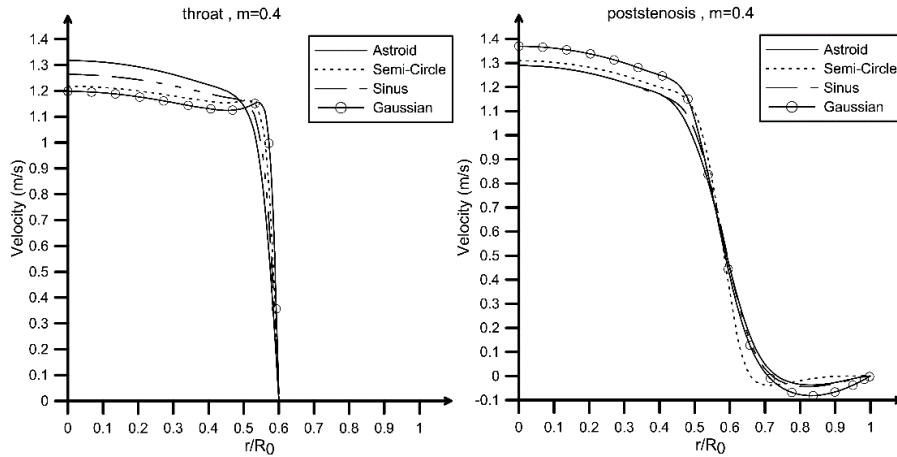


Fig. 8. Axial Velocity in all shapes of stenosis for $m=0.4$.

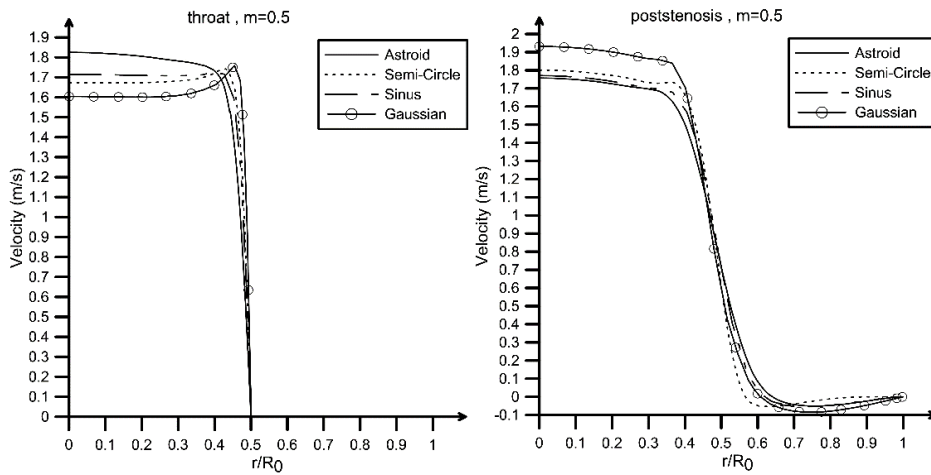


Fig. 9. Axial Velocity in all shapes of stenosis for $m=0.5$.

Table 1 Maximum wall shear stress

Stenosis Type	Stenosis Severity			Stenosis Location	Inlet Type
	0.3	0.4	0.5		
Asteroid	19.32	31.22	53.54	3R	Parabola
	21.80	32.57	54.33	3R	Flat
	19.39	31.18	53.55	5R	Parabola
	21.31	32.20	52.24	5R	Flat
Gaussian	40.06	75.91	150.5	3R	Parabola
	48.84	82.30	154	3R	Flat
	42.23	75.48	142.72	5R	Parabola
	48.60	82.00	146.6	5R	Flat
Sinus	21.30	40.14	77.79	3R	Parabola
	24.09	42.22	79.10	3R	Flat
	21.39	40.23	77.67	5R	Parabola
	23.71	41.92	78.80	5R	Flat
Circle	34.61	55.35	91.75	3R	Parabola
	41.20	59.60	93.50	3R	Flat
	34.95	55.21	92.49	5R	Parabola
	39.65	58.72	94.20	5R	Flat

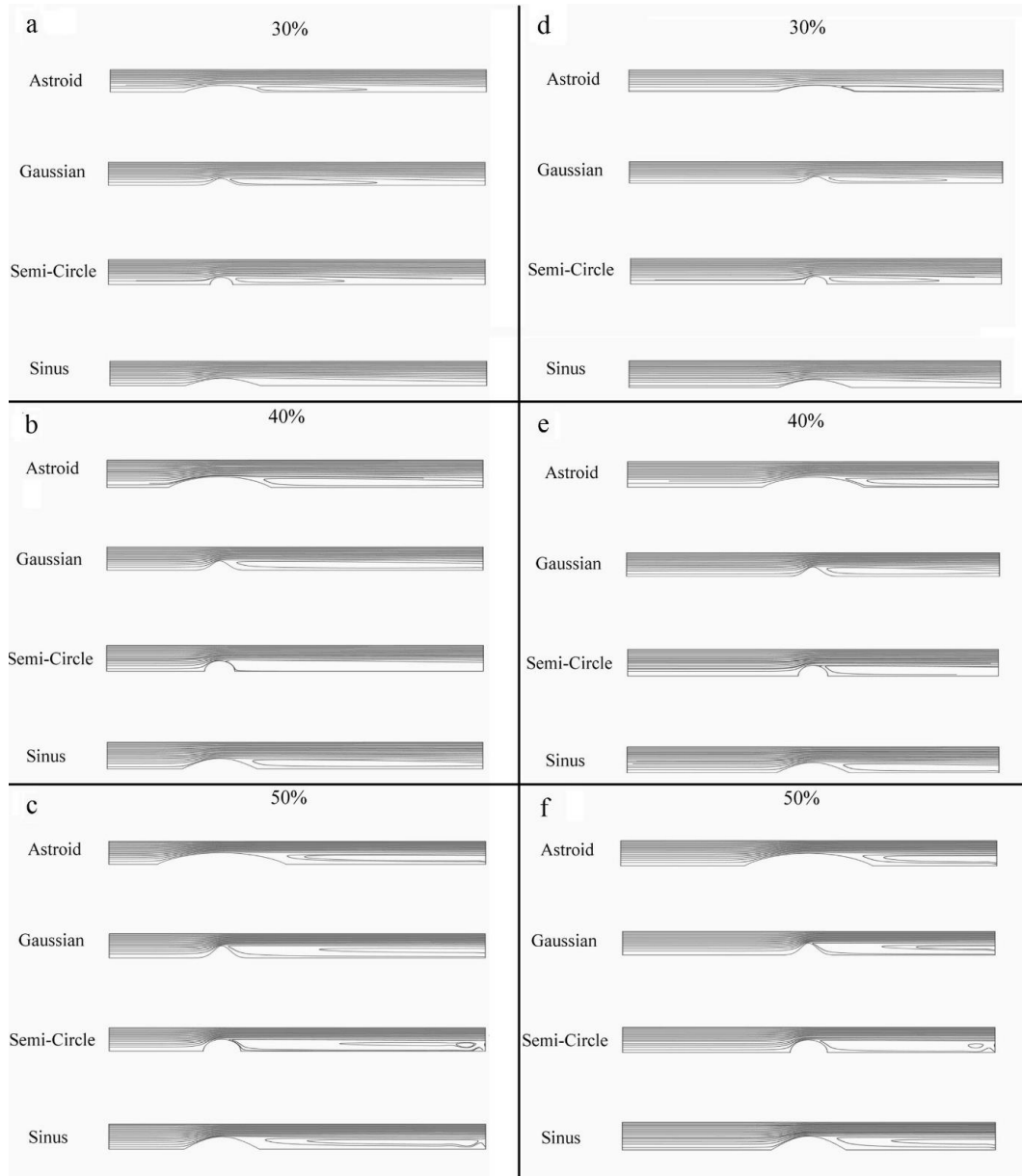


Fig. 10. Streamlines in different stenosis shapes; a) 30%-3R , b) 40%-3R, c) 50%-3R, d) 30%-5R e) 40%-5R, f) 50%-5R.

3.4 Flow Resistance

According to Poiseuille's law, flow resistance (R) is a function of the three factors of viscosity (μ), length (L), and radius (r) in a tube with internal flow.

$$R \propto \frac{\mu L}{r^4} \quad (6)$$

The above equation is not exactly valid in some arteries due to non-Newtonian properties and their small lengths. However, in this study, due to the large diameter of the artery and fully developed inlet velocity profile, the equation can be valid with a good approximation. In addition to the three above factors (viscosity, length, and radius), the shape and the severity of the stenosis can also affect the flow resistance.

The effects of these factors on maximum shear stress were studied which is defined according to Eq. (6).

$$R = \frac{\Delta p}{Q} \quad (7)$$

Viscosity, length, and radius were considered to be similar in all cases, and the variations in the resistance were only due to the stenosis' shape and severity. The data corresponding to maximum flow resistance is shown in Table 2. The letter "S" means that the maximum flow resistance occurred in about 0.2 s or systolic pressure, and the letter "LS" means that the maximum flow resistance occurred in about 0.75 s or late systolic pressure. C is defined as the ratio of stenotic flow resistance to non-stenotic flow resistance. The effects of the type of the stenosis are

Table 2 Flow resistance (MFR= Maximum Flow Resistance×10⁻⁷)

Stenosis Type	Stenosis Severity						Stenosis Location
	30%		40%		50%		
	MFR*	C	MFR	C	MFR	C	
Asteroid	3.74 (LS)	1.57	8.26 (S)	3.48	21.2 (S)	8.93	3R
	3.92 (LS)	1.65	9.25 (S)	3.89	21.9 (S)	9.22	5R
Semi-Circle	3.50 (LS)	1.47	8.47 (S)	3.57	22.1 (S)	9.30	3R
	3.70 (S)	1.56	9.46 (S)	3.98	23.1 (S)	9.73	5R
Gaussian	3.44 (LS)	1.45	9.42 (S)	3.97	25.9 (S)	10.9	3R
	4.09 (S)	1.72	10.4 (S)	4.37	26.9 (S)	11.3	5R
Sinus	3.62 (LS)	1.52	7.93 (S)	3.34	21.1 (S)	8.88	3R
	3.79 (LS)	1.60	8.85 (S)	3.73	21.7 (S)	9.13	5R

Table 3 Flow resistance (MFR= Maximum Flow Resistance×10⁻⁷)

Stenosis Type	Stenosis Severity			Stenosis Location
	0.3	0.4	0.5	
Asteroid	1.023	1.014	1.019	3R
	1.018	1.026	1.007	5R
Gaussian	1.012	1.008	1.004	3R
	0.970	1.038	1.005	5R
Sinus	1.032	1.013	1.012	3R
	1.015	1.013	1.010	5R
Semi-Circle	1.040	1.008	1.007	3R
	1.014	1.011	1.014	5R

shown in Table 2. In all cases, flow resistance was larger in 5R distance compared to the 3R distance. The largest resistance occurred at the 5R distance in the Gaussian stenosis with 50% severity, which was 11.3 times the resistance seen in the non-stenotic artery.

As mentioned earlier, blood can be assumed as a Newtonian fluid in large vessels such the carotid artery. To investigate the effect of Newtonian and non-Newtonian blood behavior on the flow characteristics, maximum shear stress values were compared in the Newtonian and non-Newtonian cases. The Carreau model suggested by Seo(Seo 2013) was used for the non-Newtonian blood. In this model, the relationship between shear rate and viscosity is as follows:

$$\frac{\mu - \mu_{\infty}}{\mu_0 - \mu_{\infty}} = \left[1 + (\lambda \dot{\gamma}^2) \right]^{\frac{(n-1)}{2}} \quad (8)$$

where, μ_0 and μ_{∞} are viscosity at zero and infinite shear rate, respectively. Their values are 0.056 kg/ms and 0.0035 kg/ms, respectively. The parameter λ is a constant with the unit of time. Its inverse represents the shear rate in which viscosity starts to decrease and is equal to 3.313 s. The parameter n is a dimensionless constant equal to

0.3568.

As can be seen in Table 3, the difference between the results obtained from non-Newtonian model and those obtained from the Newtonian model are negligible, and therefore, the Newtonian fluid assumption is acceptable here. More details about wall shear stress and velocity profiles in non-

Newtonian case could be found in supplemental material.

4. CONCLUSION

The pulsatile flow in the common carotid artery was solved using the axisymmetric flow assumption. The unsteady flow was modeled in Comsol Multiphysics and was solved using its FEM solver. To evaluate the effect of the curvature and the type of the stenosis on the maximum shear stress and the flow behavior, four different shapes of stenosis including Gaussian, semi-circle, sinus, and asteroid were simulated with 30%, 40%, and 50% stenosis severities around the artery's symmetry axis. Inlet velocity profile was assumed to be fully developed and pulsatile. The problem was solved for two wall boundary condition, *i.e.* non-slip and permeable wall. It was found that the difference between these

two modes is very small and can be neglected. Simulations were performed for two Newtonian and non-Newtonian fluids. Since the common carotid artery is relatively large, the assumption of Newtonian fluid is valid.

The results of the study show that in the four types of the stenosis, Gaussian curve has most critical condition which is true for all cases. Even in the case of 30% stenosis severity, there was a possibility of damage to the endothelial cells in the Gaussian curve, while in other three types of stenosis, there was no risk of damage to the endothelial cells in 30% stenosis severity. After Gaussian curve, semi-circle, sinus, and asteroid respectively had the largest risk of damaging the endothelial cells. In all cases, there was a risk of damage to the endothelial cells in 50% and higher stenosis severities, and there was even the risk of formation of blood clots in the Gaussian stenosis.

To evaluate the effect of location of stenosis, they were considered at the distances of 3 and 5 times the diameter from the beginning of the artery. The results showed that the location of stenosis does not affect the value of the maximum shear stress significantly. To examine the effects of the type of inlet velocity profile on the results, maximum shear stresses were compared in two cases of fully developed and flat velocity profiles. No significant difference was observed between the results of these two cases. However, the location of stenosis affected flow resistance, and as the distance of the stenosis from the beginning of the artery increased, flow resistance increased 3% to 18.5%. To further study this problem in the future, the walls can be assumed to be flexible.

REFERENCES

- Azer, K. and C. S. Peskin. (2007). A One-Dimensional Model of Blood Flow in Arteries with Friction and Convection Based on the Womersley Velocity Profile. *Cardiovascular Engineering* 7(2), 51–73.
- Fatouraee, N., X. Deng, A. Champlain and R. Guidoin (1998). Concentration Polarization of Low Density Lipoproteins (LDL) in the Arterial System. *Annals of the New York Academy of Sciences* 858(1),137–46.
- Fry, D. L. (1968). Acute Vascular Endothelial Changes Associated with Increased Blood Velocity Gradients. *Circulation Research* 22(2),165–97.
- Fung, Y. C. (2013). *Biomechanics: Motion, Flow, Stress, and Growth*. Springer Science & Business Media.
- Jahangiri, M., M. Saghafian and M. R. Sadeghi (2015a). Numerical Simulation of Hemodynamic Parameters of Turbulent and Pulsatile Blood Flow in Flexible Artery with Single and Double Stenoses. *Journal of Mechanical Science and Technology* 29(8), 3549–60.
- Jahangiri, M., M. Saghafian and M. R. Sadeghi (2015b). Numerical Study of Turbulent Pulsatile Blood Flow through Stenosed Artery Using Fluid-Solid Interaction. *Computational and Mathematical Methods in Medicine*.
- Karimi, S. *et al.* (2013). Simulation of Pulsatile Blood Flow through Stenotic Artery Considering Different Blood Rheologies: Comparison of 3D and 2D-Axisymmetric Models. *Biomedical Engineering: Applications, Basis and Communications* 25(2),1350023.
- Krejza, J. *et al.* (2006). Carotid Artery Diameter in Men and Women and the Relation to Body and Neck Size. *Stroke* 37(4), 1103–5.
- Marcinkowska-Gapińska, A., J. Gapinski, W. Elikowski, F. Jaroszyk and L. Kubisz. (2007). Comparison of Three Rheological Models of Shear Flow Behavior Studied on Blood Samples from Post-Infarction Patients. *Medical & Biological Engineering & Computing* 45(9), 837–44.
- Perktold, K., G. Karner, A. Leuprecht and M. Hofer (1999). Influence of non-Newtonian Flow Behavior on Local Hemodynamics. *ZAMM- Journal of Applied Mathematics and Mechanics/Zeitschrift Für Angewandte Mathematik Und Mechanik* 79(1), 187–90.
- Ramstack, J. M., L. Zuckerman and L. F. Mockros (1979). Shear-Induced Activation of Platelets. *Journal of Biomechanics* 12(2), 113–25.
- Razavi, A., E. Shirani and M. R. Sadeghi. (2011). Numerical Simulation of Blood Pulsatile Flow in a Stenosed Carotid Artery Using Different Rheological Models. *Journal of Biomechanics* 44(11), 2021–30.
- Sadeghi, M. R., E. Shirani, M. Tafazzoli-Shadpour and M. Samaee (2011). The Effects of Stenosis Severity on the Hemodynamic Parameters—assessment of the Correlation between Stress Phase Angle and Wall Shear Stress. *Journal of Biomechanics* 44(15), 2614–26.
- Seo, T. (2013). Numerical Simulations of Blood Flow in Arterial Bifurcation Models. *Korea-Australia Rheology Journal* 25(3),153–61.
- Sugihara-Seki, M. and M. Fu. Bingmei (2005). Blood Flow and Permeability in Microvessels. *Fluid Dynamics Research* 37(1), 82–132.
- Wake, A. K. (2005). Modeling Fluid Mechanics in Individual Human Carotid Arteries.